

Transport Mechanisms in Oil Shale Drying and Pyrolysis

Bronwyn L. Duffy[†] and Brian S. Haynes*

Department of Chemical Engineering, University of Sydney, N.S.W., 2006, Australia

Received April 6, 1992. Revised Manuscript Received September 4, 1992

Drying and retorting rates of Australian oil shales are limited by the low permeability of the rock matrix. This paper reports an experimental study of the mechanisms of gas transport in oil shales of the Stuart/Rundle (Kerosene Creek) and Condor deposits. The dominant transport mechanism for gas transport through the raw rock matrix is Knudsen diffusion, with an average effective air diffusivity for transport parallel to the bedding plane in Stuart oil shale of $7.3 \times 10^{-8} \text{ m}^2\text{s}^{-1}$ at 295 K; for Condor oil shale, this value is $9.5 \times 10^{-8} \text{ m}^2\text{s}^{-1}$. These values are close to those predicted from measured pore size distributions if a tortuosity factor of about 8 (± 3) is assumed. It is also in reasonable agreement with the value determined from drying kinetics, and it is therefore possible to predict drying kinetics from routine room-temperature permeability measurements. The sedimentary rock is highly anisotropic, with the diffusivity normal to the bedding plane in Stuart oil shale being just $5.7 \times 10^{-9} \text{ m}^2\text{s}^{-1}$. Retorting leads to the development of a more open pore structure, with the permeability of the matrix being enhanced by higher retorting temperatures. Gas is transported through retorted oil shale by a combination of Knudsen diffusion and viscous flow.

Introduction

Australian oil shales, such as those of the Rundle/Stuart and Condor deposits, are characterized by a high moisture content, of the order of 10 wt % even after air drying. The removal of this moisture imposes penalties both in terms of processing time and energy requirements for the retorting operation.

We have previously studied the kinetics of drying of oil shales from the Stuart deposit over the temperature range 100–250 °C and have shown that drying proceeds as a receding front through the relatively impermeable oil shale matrix, with the sharp front separating regions of dried and undried material.¹ The drying kinetics of the oil shale are now determined by the transport properties of the dried region as moisture evaporating at the interface moves through the dried region. The saturation vapor pressure of water at the interface temperature provides the driving force for transport from the interface to the exterior of the sample.

Based on the observed drying kinetics, the transport properties of the Stuart oil shale could be described in terms of an effective Knudsen diffusivity, $D_{K,\text{eff}}$, for steam at 175 °C, of $2.1 (\pm 0.6) \times 10^{-7} \text{ m}^2\text{s}^{-1}$. This value showed little variation between samples from the same seam (Kerosene Creek member) and appears to represent a fundamental property of the shale matrix.¹ The concept of the receding evaporation front has been applied also to the drying of Condor oil shale and found to be appropriate there too.² The value of the effective Knudsen diffusivity for transport in this rock was found to be $1.6 (\pm 0.5) \times 10^{-7} \text{ m}^2\text{s}^{-1}$.

The geology of the various Queensland Tertiary oil shale sediments, including those of the Rundle/Stuart and

Condor deposits, is broadly similar. The similarity in the effective transport coefficients for the two deposits studied may therefore be expected to extend to all of the Queensland Tertiary oil shales.

Transport processes can also be expected to influence the extraction of the organic kerogen material during pyrolysis of oil shales, typically at temperatures in the range 400–650 °C. Do and Bell³ have developed a transport model which relates the removal of the organic material during retorting with changes in the pore structure of the shale matrix, the tortuosity, and pore size varying with the extent of pyrolysis. Guindy et al.⁴ have found evidence for a diffusion-limited gas production in oil shale pyrolysis.

The measurement of drying kinetics for the determination of the transport properties of the oil shales is experimentally demanding. Other approaches to obtaining these properties, such as characterization of the porous structure by surface area or porosimetry measurements, are model dependent and are not known for their absolute reliability. Therefore, in this paper we investigate the use of routine permeability measurements to determine the mechanisms of gas transport in Queensland Tertiary oil shales and we demonstrate the application of this simple method to the prediction of the transport kinetics of the drying and pyrolysis processes.

Experimental Section

Routine permeability measurements, similar in principle to those described by Pirson,⁵ were conducted on dried and on retorted shale samples, in order to investigate the transport of gases during drying and retorting, respectively.

Rectangular prisms ($\sim 8 \times \sim 8 \times \sim 30 \text{ mm}$) were cut from air-dried samples of Stuart or Condor oil shale in such a way that the clearly observed bedding planes of the sample were either parallel to the end ($8 \text{ mm} \times 8 \text{ mm}$) faces of the prism or normal

* Author for correspondence at above address. Tel: 61-2-692.3435. Fax: 61-2-692.2854. email: haynes@cerisc.ce.su.oz.au.

[†] Presently at Division of Coal and Energy Technology, C.S.I.R.O., North Ryde, N.S.W., 2113, Australia.

(1) Lane, D.; Ramjas, S.; Haynes, B. S. *Fuel* 1988, 67, 1321–1326.

(2) Batta, J. L.; Ramjas, S.; Haynes, B. S. *Proc. 17th Australasian Chem. Eng. Conf.* 1989, 259.

(3) Do, H.; Bell, P. R. F. *Chem. Eng. Commun.* 1989, 78, 179.

(4) Guindy, N. M.; El-Akkad, T. M.; Flex, N. S.; El-Massary, S. R.; Nashed, S. *Thermochim. Acta* 1985, 85, 211.

(5) Pirson, S. J. *Oil Reservoir Engineering*, 2nd ed.; McGraw-Hill: New York, 1958.

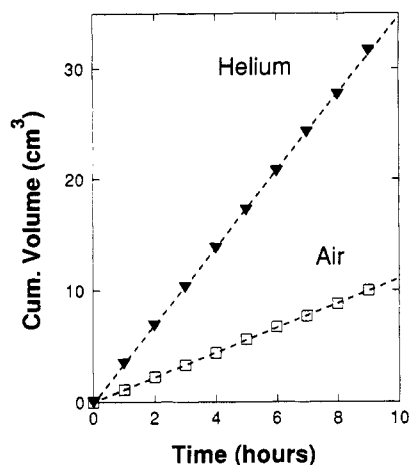


Figure 1. Experimental results for the flow of helium and air parallel to the bedding planes in dried Stuart oil shale subjected to an upstream pressure of 360 kPa ($p_m = 260$ kPa).

to those faces. The cut sample was predried in air at 110 °C for 24 h; some samples were additionally reported in a N_2 -fluidized bed for 60–90 min at either 500 or 650 °C. The sample was then mounted in epoxy resin encased in tubular metal supports. Great care was taken here to ensure that the 8×8 mm faces of the samples were not covered or in any way contaminated by the epoxy resin; equally great care was taken to ensure an intimate contact of the epoxy with the long faces of the sample and with the wall of the tubular support in order to prevent gas bypassing the encased sample.

The permeability measurements were conducted by applying a constant pressure (in the range of 200–750 kPa) of either air or helium to one end of the sample and collecting the gases leaving the other end at atmospheric pressure (~ 100 kPa). The cumulative volumes of gas which passed through the ~ 30 mm length of the sample were measured over a period from 1 to 8 h in order to determine the steady-state gas flow rates.

Results

Typical results for the cumulative volume of gas collected versus time are shown in Figure 1 for the permeation, parallel to the bedding planes, of both helium and air through dried, unretorted Stuart oil shale. The same sample was employed in both experiments and the differences in slopes of the lines reflect the relative rates of mass transfer of helium and air through unretorted oil shale, without any influence of intersample variation. Indeed, such variations were found to be very slight among the samples studied.

In Figure 2, data for the transport of air parallel to the bedding planes of a dried, unretorted shale sample are compared with data, obtained for a separate sample but under otherwise identical conditions, for transport normal to the bedding planes.

Discussion

Mechanism of Gas Transport. Descriptions of multicomponent gas transport in porous media generally invoke three independent mechanisms: Knudsen diffusion in which the resistance to mass transfer is due to collision of the molecules with the walls of the porous medium, and in which components move under the influence of their own partial pressure gradient; viscous or bulk flow in which the gas acts as a continuum fluid driven by a total pressure gradient; and ordinary diffusion in which the different

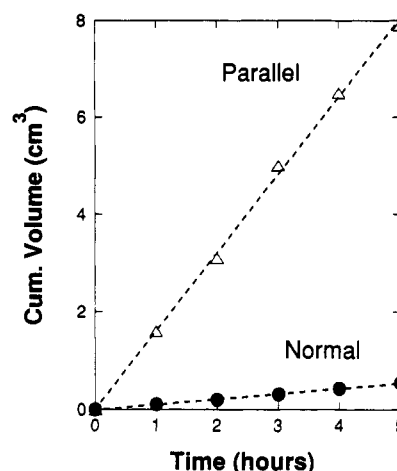


Figure 2. Experimental results for dried Stuart oil shale samples for the flow of air either parallel or normal to the bedding plane. The upstream pressure was 300 kPa ($p_m = 200$ kPa).

species of a mixture move relative to each other under the influence of a mole fraction gradient.

For a single-component gas, the Knudsen diffusion and viscous flow mechanisms prevail and the total molar flux, N , is given by⁶

$$\tilde{N} = -D_{K\text{eff}} \tilde{\nabla} c - \frac{cB}{\mu} \tilde{\nabla} p \quad (1)$$

According to the dusty gas model of transport through porous media,⁶ the Knudsen diffusion coefficient represents a binary interaction between gas molecules and large "dust" particles which represent the walls of the pores and it is not necessary that Knudsen flow conditions be established for eq 1 to apply and for an effective Knudsen diffusivity to be apparent.

For an isothermal porous plug of cross-sectional (flow) area A , and length L , eq 1 becomes, for an ideal gas obeying $p = cRT$,

$$n = \frac{A}{RTL} \left[D_{K\text{eff}} \Delta p + \frac{B}{2\mu} \Delta p^2 \right] \quad (2)$$

or

$$\frac{n}{\Delta p} = \frac{A}{RTL} \left[D_{K\text{eff}} + B \frac{p_m}{\mu} \right] \quad (3)$$

where Δp is the pressure differential across the sample and p_m is the mean of the upstream and downstream pressures.

The contributions of Knudsen diffusion and viscous flow can now be identified by plotting $n/\Delta p$ vs p_m . For transport limited by Knudsen diffusion, the quantity $n/\Delta p$ should be constant. Any contribution by viscous flow will be apparent from a linear dependence of $n/\Delta p$ on p_m . A typical plot of data obtained for air permeation through a dried sample of Stuart oil shale is given in Figure 3. The dashed lines in Figure 3 represent ± 2 standard deviations about the mean and it is concluded that there is no significant dependence on the mean pressure, indicating that Knudsen diffusion is the dominant transport mechanism.

A total of six Stuart samples and four from the Condor deposit were studied for air flow parallel to the bedding planes. The average effective Knudsen diffusion coefficient

(6) Mason, E. A.; Malinauskas, A. P. *Gas Transport in Porous Media: The Dusty Gas Model*; Elsevier Science Publishers B.V.: Amsterdam, 1984.

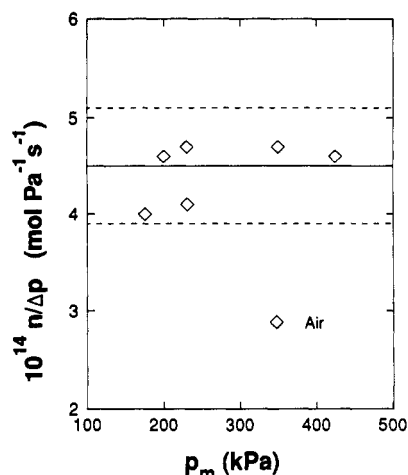


Figure 3. Experimental data for in-plane transport of air through dried Stuart oil shale, plotted according to eq 3.

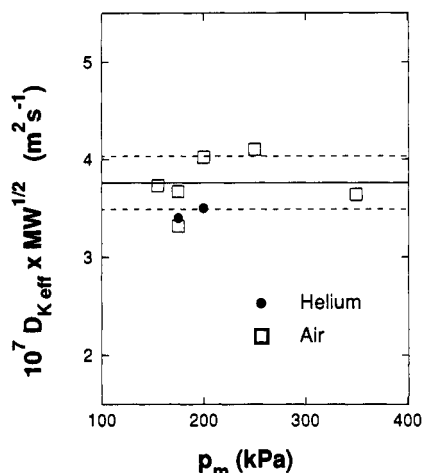


Figure 4. Verification of the molecular weight dependence of the in-plane Knudsen diffusion coefficients for air and helium.

coefficients obtained by this analysis were $7.3 \times 10^{-8} \text{ m}^2 \cdot \text{s}^{-1}$ (Stuart) and $9.5 \times 10^{-8} \text{ m}^2 \cdot \text{s}^{-1}$ (Condor), each with a relative standard deviation less than 20%. As found previously, there is little evidence of intersample variation.

Further evidence that Knudsen diffusion controls transport in these samples is provided by a comparison of the transport rates of helium and air. The apparent Knudsen diffusivity of different gases in a porous medium varies as⁶

$$D_{K\text{eff}} \approx \text{constant} \cdot \left[\frac{T}{M_w} \right]^{1/2} \quad (4)$$

As shown in Figure 4 for helium and air transport through a single sample of Stuart oil shale, the molecular weight dependence expected for Knudsen diffusion is verified in that the quantity $D_{K\text{eff}} M_w^{1/2}$ is constant at the constant temperature of the experiments.

Our earlier analysis of the drying kinetics of oil shale at temperatures from 100 to 250 °C, corresponding to mean pressures from 50 to 1500 kPa, also showed the in-plane transport rates to be controlled by Knudsen diffusion, with an average Knudsen diffusivity for steam of $2.1 (\pm 0.6) \times 10^{-7} \text{ m}^2/\text{s}$. Based on the present measurements of the air diffusivity at room temperature, eq 4 can be used to provide an estimate of the Knudsen diffusivity of steam in the dried oil shale matrix at 175 °C of $1.2 (\pm 0.2) \times 10^{-7} \text{ m}^2 \cdot \text{s}^{-1}$, which is in remarkably good agreement with the drying result. For Condor shale, the values are $1.6 (\pm 0.5)$

$\times 10^{-7} \text{ m}^2 \cdot \text{s}^{-1}$ from the drying experiments and $1.5 (\pm 0.3) \times 10^{-7} \text{ m}^2 \cdot \text{s}^{-1}$ based on the present permeability measurements and eq 4. Thermomechanical effects, such as pore expansion and loss of crystalline water at the higher temperatures of the drying experiments, may be expected to give rise to a small discrepancy between the estimates, but these effects are clearly not great.

Predicting the Effective Diffusivity. A structural model must be assumed in order to be able to predict diffusivities from measurements of structural parameters. For free-molecular flow in a medium containing cylindrical capillaries of radius r_p , the effective Knudsen diffusion coefficient is given by

$$D_{K\text{eff}} = \eta D_K = \frac{2}{3} \eta r_p \left[\frac{8RT}{\pi M_w} \right]^{1/2} \quad (5)$$

where the diffusibility, η , is generally expressed as

$$\eta = \epsilon / \tau \quad (6)$$

The distribution of pore radii in raw Stuart and Condor oil shales has been reported⁷ to give volume-mean radii of 12.9 nm and 7.9 nm, respectively, although it should be noted that, in both cases, the distribution is rather broad and that these mean values should probably be treated more as characteristic only. Nevertheless, when these radii are compared with the mean free path of gas molecules under our typical experimental conditions (21 nm for air at $p = 300 \text{ kPa}$ and room temperature) it is clear that free-molecular flow conditions are not generally established.

Comparison of eqs 4 (the dusty gas model) and 5 reveals that eq 5 is, in terms of the dusty gas model, quite general, without limitation as to the Knudsen number prevailing in the pores. Therefore, we can use our experimental results and the volume-mean pore radii cited above to estimate $\tau = 11$ for Stuart and $\tau = 5$ for Condor oil shales if we assume a porosity of 20% in each case.

The value of the tortuosity, τ , is generally expected to be 3 for randomly oriented pores, or of the order of 4–9 if directional autocorrelation effects are accounted for.⁸ Most experimental values lie within the limits 3–9, and the present results would appear to be consistent with these results. However, it should be noted that the anisotropy observed with these samples restricts the directional degrees of freedom for diffusion to 2, and the expected values of τ could therefore be expected to lie between 2 and 6. Despite this, the agreement between our experimental results and expectation remains reasonable; i.e., the Knudsen diffusivity of the samples is predictable within a factor of 2 from measurements of mean pore structure.

Anisotropy of the Transport Characteristics. The average Knudsen diffusivity for transport normal to the bedding planes of Stuart oil shale was found to be $5.7 \times 10^{-9} \text{ m}^2 \cdot \text{s}^{-1}$, more than a factor of 10 less than the value for parallel diffusion. This pronounced anisotropy has implications for the processing of oil shales because the characteristic size for the processing of a lump of shale must take into account the disposition of the bedding planes to the lump shape; i.e., the characteristic drying or retorting time of the sample will be determined more by the dimension of the particle parallel to the bedding plane

(7) Gannon, A. J.; Duffy, G. J.; Wall, G. C. *Integrated Processing of Australian Oil Shale*; NERDDP Project No. 1165; Final Report, 1990; p 6.

(8) Bhatia, S. K. *J. Catal.* 1985, 93, 196.

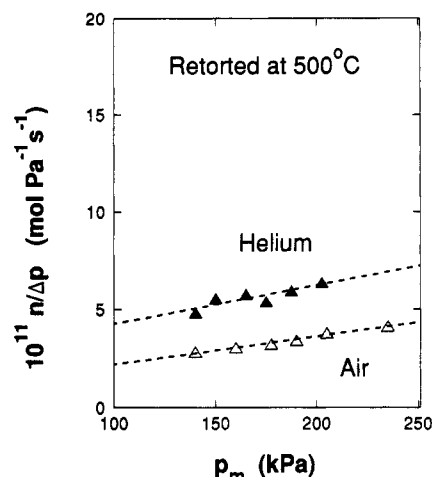


Figure 5. Experimental data for the in-plane flow of helium and air through Condor oil shale previously retorted at 500 °C.

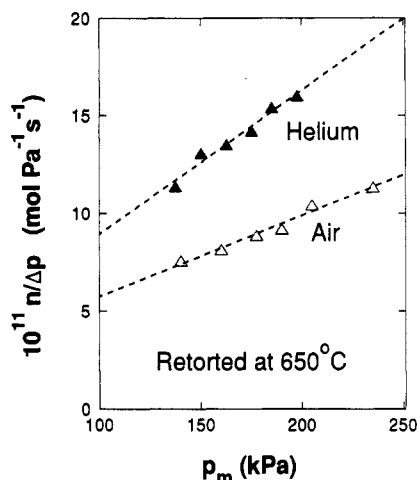


Figure 6. Experimental data for the in-plane flow of helium and air through Condor oil shale previously retorted at 650 °C.

than by the normal dimension. In other words, the characteristic dimension for transport may not be well represented by measures such as sieve size or particle volume and a detailed understanding of the fracture mechanics of the rock is required to complement the transport modelling.

The clay minerals, smectite and kaolinite, have been found to comprise from 20 to 50 wt % of Stuart oil shale⁹ and similar mineralogy applies to all of the Queensland Tertiary oil shales. These minerals are described as having "corn-flake" and pseudo-hexagonal plate structures, respectively,¹⁰ and form the "continuous phase" in the rock matrix which also includes impermeable inclusions such as quartz and feldspars. It is presumably their parallel orientation during sedimentation and compaction in a lacustrine environment which gives rise to the pronounced fissility and transport anisotropy of the rock.

Retorted Shale. Flow rates parallel to the bedding planes in retorted Condor shale are approximately 3 orders of magnitude higher than through raw oil shale, as shown in Figures 5 and 6 for plots of permeation rates according to eq 3 ($n/\Delta p$ vs p_m). The existence of a marked dependence of the flow rate on mean pressure indicates

Table I. Summary of Results Obtained from Figures 5 and 6, Using Eqs 3 and 6, for the In-Plane Transport Properties of Retorted Condor Oil Shale

retorting temp, °C	permeation gas	$10^5 D_{K\text{eff}}$, $\text{m}^2\cdot\text{s}^{-1}$	$10^{15} B$, m^2	ϵ/τ	r_p , nm
500	air	0.9	2.9	0.038	790
	helium	2.6	4.1	0.029	1070
650	air	1.4	6.5	0.039	1150
	helium	1.4	11.5	0.003	5500

a major contribution from viscous flow, especially in the sample retorted at 650 °C.

The diffusive and viscous flow parameters are related via the structural characteristics of the medium⁶

$$\frac{\epsilon}{\tau} = \frac{9D_{K\text{eff}}}{32b^2B}, \quad r_p = \left[\frac{8B}{\epsilon/\tau} \right]^{1/2} \quad (7)$$

Table I summarizes the results obtained from Figures 5 and 6 for the various parameters; the 95% confidence intervals for the various parameters are as large as 100% of the parameter value, owing to the large extrapolation of the raw data to zero mean pressure. Nevertheless, some significant trends emerge. In most cases, the experimentally obtained diffusibility is of the order of the value expected: e.g., for "standard" values of $\epsilon = 0.20$, $\tau = 7$, the expected diffusibility factor is $\eta = 0.029$. For helium permeation of the material retorted at 650 °C, the diffusibility factor is anomalously low (and the effective pore radius is correspondingly high), chiefly as a result of the low value of the Knudsen diffusion coefficient obtained for these conditions.

The values of the effective pore radius calculated from the data are higher than values obtained from porosimetry measurements on retorted Condor shale⁷ which gave pore sizes in the range 5–500 nm with a volumetric mean pore radius of 30 nm. However, it should be noted that the porosimetry measurements⁷ were carried out on spent shale prepared by modified Fischer assay; this slow-heating technique greatly promotes secondary pyrolysis of the products of kerogen decomposition which may give rise to a partially blocked pore structure. The present results indicate a substantially increased permeability when more rapid retorting (650 vs 500 °C) is carried out.

Conclusions

The dominant mechanism for gas transport through unretorted oil shale is Knudsen diffusion. The average effective air diffusivities obtained for transport parallel to the bedding plane in Stuart and Condor oil shale were $7.3 (\pm 1.3) \times 10^{-8}$ and $9.5 (\pm 1.7) \times 10^{-8} \text{ m}^2\cdot\text{s}^{-1}$, respectively. There is very little intersample variation apparent in these determinations. The values obtained for the effective Knudsen diffusivity are consistent with mean pore radii based on mercury porosimetry if tortuosities in the range 5–11 are adopted.

The Knudsen diffusivity of $5.7 \times 10^{-9} \text{ m}^2\cdot\text{s}^{-1}$ for transport normal to the bedding plane in Stuart oil shale indicates the significant anisotropic nature of the oil shales. This result has implications for the modeling of transport rates from randomly shaped oil shale samples as the characteristic dimension for transport may not be well represented by measures such as sieve size or particle volume.

The measured values of the effective Knudsen diffusivity for air and helium at room temperature can be extrapolated

(9) Patterson, J. H.; Hurst, H. J. *Proc. 5th Australian Workshop on Oil Shale, Lucas Heights 1989*, 189.

(10) Wigge, P. K. C. In *The Structure and Properties of Porous Materials*; Everett, D. H., Stone, F. S., Eds.; Butterworths Scientific Publications: London, 1958.

to yield estimates for water vapor transport rates under rapid drying conditions (temperatures up to 250 °C) which are in excellent agreement with earlier direct measurements of those rates. Routine permeability measurements, which are quick and inexpensive, can therefore be used to predict the drying kinetics of oil shale samples for design and process control purposes.

Gas is transported through retorted oil shale by a combination of Knudsen diffusion and viscous flow. The effect of retorting is to open out the pore structure considerably, but more work is required to quantify and generalize these observations.

Acknowledgment. This work was supported by Southern Pacific Petroleum N.L.

Glossary

A	sample cross-sectional area, m^2
B	permeability, m^2
c	molar gas concentration, $\text{mol}\cdot\text{m}^{-3}$
D_K	Knudsen diffusivity, $\text{m}^2\cdot\text{s}^{-1}$
L	sample length, m
M_w	molecular weight, $\text{kg}\cdot\text{mol}^{-1}$
n	molar gas flow, $\text{mol}\cdot\text{s}^{-1}$
N	molar gas flux, $\text{mol}\cdot\text{m}^{-2}\cdot\text{s}^{-1}$
p	gas pressure, Pa
r_p	pore radius, m
R	gas constant, $8.314\text{ J}\cdot\text{mol}^{-1}\cdot\text{K}^{-1}$
T	temperature, K
U	mean speed, $(8RT/\pi M_w)^{1/2}$, $\text{m}\cdot\text{s}^{-1}$
ϵ	porosity
η	diffusibility
μ	gas viscosity, $\text{Pa}\cdot\text{s}$
τ	tortuosity